Bulletin of the Seismological Society of America. Vol. 56, No. 2, pp. 441–454. April, 1966

VELOCITY FILTERING OF SEISMIC CORE PHASES

By W. J. Hannon* and R. L. Kovach*

ABSTRACT

Recent studies have proposed complexities in the velocity-depth function for the region surrounding the inner core which require additional branches in the travel time curve for *PKP* in the epicentral range of 125° to 160°. The proposed *PKP* arrivals can be separated on the basis of their apparent velocities, which range from 24 km/sec to 100 km/sec. Using the Tonto Forest array in Arizona coupled with adjoining LRSM stations in the western United States, an effective linear array of 400 km in size is attained. Data from several events in the distance range from 130° to 160° recorded on this array have been velocity filtered and show some evidence of two precursors to *PKP* in the distance range from 135° to 143° and at least one intermediate branch between PKP_1 and PKP_2 at distances greater than 143°. The results appear to support the velocity solution for the core proposed by Adams and Randall, although more data are required before a conclusive discrimination can be made between competing velocity models.

Introduction

The presence of a small, possibly solid, inner core with a radius of about 1250 km was proposed by Lehmann in 1936 to explain observations of *PKP* phases in the shadow zone. This hypothesis was adopted by both Gutenberg and Richter (1938) and Jeffreys (1939 a, b). The velocity models proposed by these investigators were quite similar in the interior of the inner core, but differed markedly in the transition zone at the boundary of the inner core. At present, the nature of this boundary is still open to speculation and the existence of shear waves in the inner core has not been established.

As the quantity and quality of seismological data have increased, various investigators (Gutenberg, 1957, 1958 a, b, 1959; Hai, 1961, 1963; Bolt, 1962, 1964; Adams and Randall, 1963, 1964) have observed events which appear to be core phases that are not explained by the original velocity models of Jeffreys and Gutenberg and Richter. In particular, arrivals preceding the main *PKP* phase have been observed at distances less than 140° and triplication of *PKP* has been noted beyond 143°. Because of these observations, various modifications to the early velocity models have been proposed (Figure 1).

Since the observed core arrivals are separated by less than 15 seconds over most of their observable range, it is difficult to use travel time data alone to examine the validity of the proposed models. Furthermore, variations in the relative amplitudes of the different phases and uncertainty as to which phase is the first arrival

* W. J. H. now at Department of Earth Sciences, Washington University, St. Louis. R. L. K. now at Department of Geophysics, Stanford University, Stanford, California.

in certain distance ranges, complicate the problem. When the uncertainties due to multiple phases from shallow focus earthquakes, and possible errors in epicenter locations, depth of foci, and origin time are also considered, it is necessary that criteria other than travel times be used for phase identification.

One such criterion is the slope of the travel time curve or the apparent surface velocity. The apparent velocities for the various *PKP* arrivals are considerably

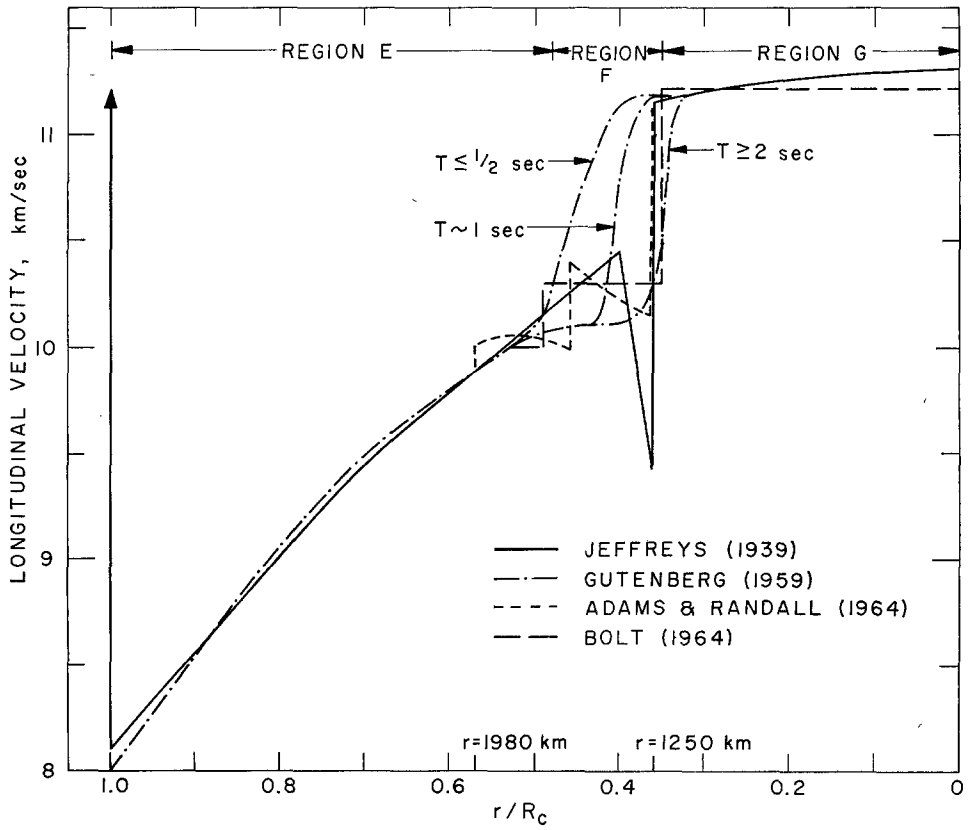

FIG. 1. Proposed longitudinal velocity distributions in the earth's core. The velocity distribution proposed by Hai (1963) is similar to that of Gutenberg for $T > 2$ sec with the addition of two small regions with negative gradient at $r/R_c = 0.36$ and 0.54.

different, ranging from 24 km/sec to over 100 km/sec. A large array of seismographs can be used to employ velocity filtering as a technique of phase identification. We have used the Tonto Forest (TFO) crossed array in Arizona combined with surrounding portable Long Range Seismic Measurement (LRSM) stations to form an array of about 400 km in linear dimension. The use of velocity filtering as a method of phase identification is not new, but this is the first time that it has been applied to the analysis of phases emerging from the transition zone at the boundary of the inner core.

Theoretical Travel Times and Apparent Velocities

The most important differences in the velocity models occur at the transition zone between the inner and outer core (Figure 1). The familiar Jeffreys (1939 b) solution has a transition region with a large negative velocity into the inner core. Gutenberg's (1958 b) model has a frequency-dependent velocity distribution which gives the increase in velocity without the region of negative velocity gradient. The modification of Jeffreys' model proposed by Adams and Randall (1964) has three discontinuous velocity increases joined by regions with small negative velocity

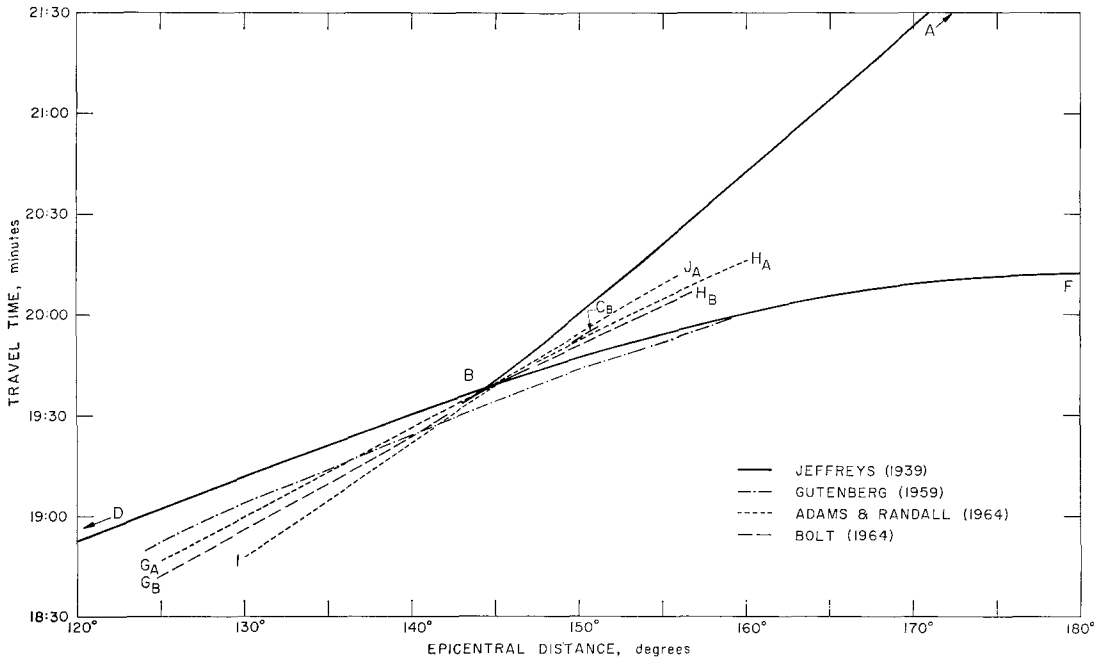

FIG. 2. Travel time curves for *PKP*. Hai's model has a branch combining features of *IJ* from 137° to 143° and *GH* from 143° to 157°. It also has a short period precursor similar to Gutenberg in the range 128° to 137°.

gradients; whereas, the model proposed by Bolt (1962) has two discontinuous velocity increases joined by a region of constant velocity. Hai's (1963) model is not shown in Figure 1 but it is quite similar to the $T \geqq 2$ second solution of Gutenberg except for a small dip in the velocity at a radius of about 1920 km.

The distinctive features of the various travel time curves predicted by these models are compared to the familiar Jeffreys model in Figure 2. We shall follow the notation proposed by Adams and Randall (1964) for the various *PKP* arrivals. The two main branches P'_{AB} and P'_{DF} are quite similar for all the models. Jeffreys' solution has a cusp at 143° followed by a short branch P'_{BC} from 143° to 147°. Gutenberg's model also has a caustic at 143°, but the branch P'_{BC} extends to distances greater than 160°. The most distinctive feature of the travel time curve for Guten-

berg's model, however, is the presence of a short period (about 1 second) precursor which arrives 3 to 10 seconds earlier than P'_{DF} at distances less than 143°.

The modification proposed by Bolt (1964) predicts a precursor P'_{GH} before P'_{DF} at distances less than 143°. This precursor becomes an intermediate phase between P'_{DF} and P'_{AB} at distances from 146° to 156°. The cusp at B is preserved and P'_{BC} extends to approximately 152°. On the other hand, Adams and Randall's (1964) solution has two precursors (P'_{IJ} and P'_{GH}) to P'_{DF} at distances less than 143°.

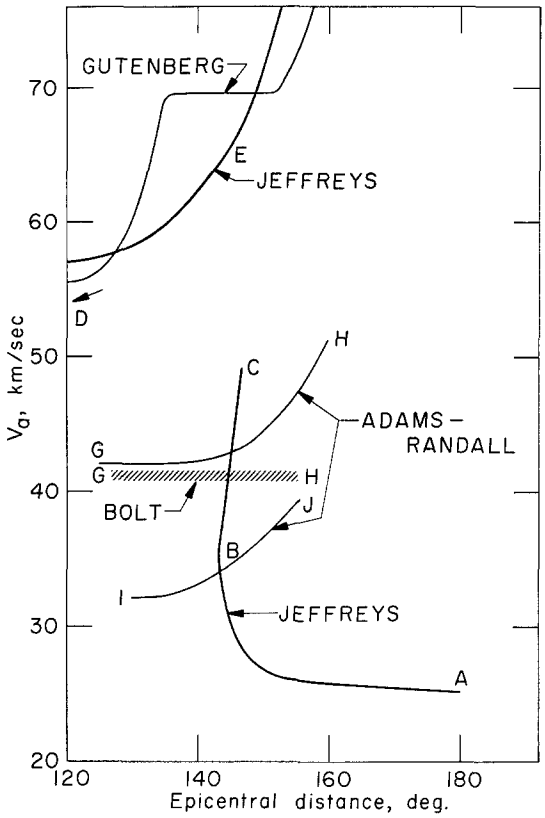

FIG. 3. Apparent surface velocities for the proposed core phases.

The first of these, P'_{IJ}, precedes the main P'_{DF} arrival by more than 17 seconds at distances less than 134°. The later precursor P'_{GH} is very similar to that predicted by Bolt's model. In addition to having two precursors, the Adams and Randall travel time curve is unique, in that it has no cusp at 143° and P'_{IJ} replaces P'_{BC} at distances greater than 143°. The excellent observational data of Hai (1963) indicate a precursor to P'_{DF} by about 12 seconds at 137°. His data also support the extension of P'_{BC} to 157°.

Figure 3 shows the apparent surface velocities for the proposed phases. The velocities for the phases are considerably different except for the proposed *GH* and *IJ* branches. Thus, with even a few stations in an array, it is relatively easy to identify P'_{AB} and P'_{DF}. It is then a simple matter to locate other phases with

respect to these arrivals. If a more dense array is available, it may be possible to identify P'_{IJ} and P'_{GH} from their apparent surface velocities.

Observational Data

The Tonto Forest linear crossed array (TFO), when combined with adjacent Long Range Seismic Measurement (LRSM) stations forms an effective large array 400 km in dimension. Figure 4 and Table 1 show the locations and coordinates of

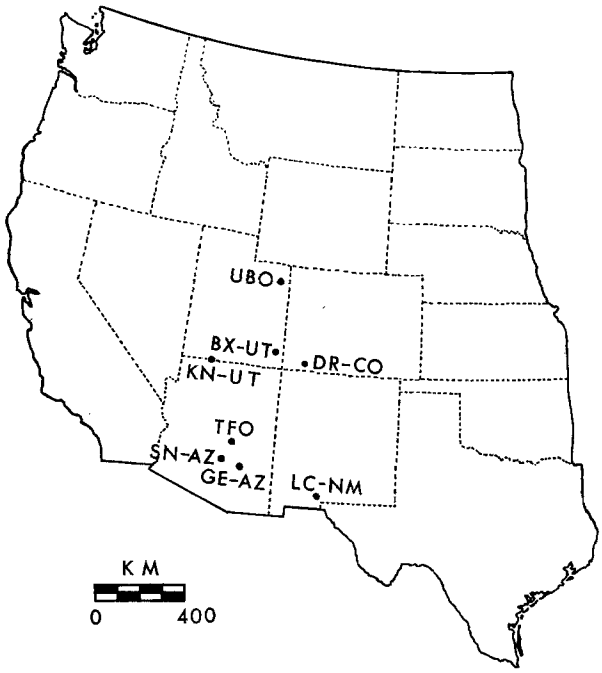

Fig. 4. The locations of the Tonto Forest array and surrounding LRSM stations in the western United States.

the stations used. TFO operates Johnson-Matheson short period seismometers at magnifications of about 500,000 at a period of 1 second. The surrounding LRSM stations operate short period Benioff seismometers at gains from $\frac{1}{3}$ to $\frac{1}{4}$ those at TFO. Both horizontal and vertical seismometers are installed at many of these sites. However, only vertical instruments were used in this study since the angles of incidence at the free surface are less than 20° for the phases analyzed.

From the events recorded at TFO, we selected 15 earthquakes (Table 2) which had particularly well defined core phases. For six of these earthquakes the corresponding LRSM records together with the records from other array stations were examined. The recording stations used corresponding to the events listed in Table 2 are given in Table 3. Sample seismograms showing typical core phases recorded at TFO are shown in Figure 5. The top two traces correspond to events 5 and 13 from Sumatra (Δ = 132.7°) and Java (Δ = 135.1°), respectively. Although the epicentral distances of the two events differ by only 3° and the focal depths are about

the same, the two records differ considerably. The Java earthquake has a precursor, possibly corresponding to the P'_{IJ} branch of Adams and Randall, but this event is not observable on seismograms of the Sumatra earthquake recorded at distances of about 132°. This difference cannot be explained on the basis of magnitude since

TABLE 1

COORDINATES OF RECORDING STATIONS

Station Code	Station Name	N. Latitude	W. Longitude
BMO	Blue Mountain	44°50′56″	117°18′20″
BX-UT	Blanding	37°33′48″	109°26′05″
DR-CO	Durango	37°27′53″	107°47′00″
GE-AZ	Globe	33°46′32″	110°31′41″
JR-AZ	Jerome	34°49′32″	111°59′25″
KM-CL	Kramer	34°52′52″	117°15′24″
KN-UT	Kanab	37°01′22″	112°49′39″
LC-NM	Las Cruces	32°24′08″	106°35′58″
LG-AZ	Long Valley	34°24′28″	111°32′45″
SN-AZ	Sunflower	33°51′49″	111°41′34″
TFO	Tonto Forest	34°17′12″	111°16′03″
UBO	Uinta Basin	40°19′18″	109°34′07″
WMO	Wichita Mts	34°43′05″	98°35′21″
WO-AZ	Winslow	34°52′53″	110°37′15″

TABLE 2

LIST OF EARTHQUAKES USED

Event No.	Date	Time	Lat. (deg)	Long. (deg)	Depth (km)	Magn.	Region
1*	1963 Sept 25	$07^h03^m54.8^s$	16.6S	28.6E	33	6.0	Northern Rhodesia
2*	1963 Oct 24	$07^h26^m25.8^s$	5.0S	102.8E	70	6.2	Sumatra
3*	1964 Feb 24	$09^h52^m18.6^s$	7.2S	67.9E	33	5.2	Chagos
4*	1964 Feb 25	$00^h34^m31.5^s$	44.6S	37.2E	33		Prince Edward Island
5	1964 Apr 2	$01^h11^m55.0^s$	5.8N	95.6E	132	6.7	Sumatra
6*	1964 Apr 3	$04^h12^m39.7^s$	3.9N	96.6E	52	6.1	Sumatra
7*	1964 Apr 8	$08^h08^m11.7^s$	6.7S	68.9E	33	6.3	Chagos
8*	1964 July 13	$23^h43^m46.3^s$	48.2S	31.5E	33		Prince Edward
9*	1964 Aug 18	$11^h09^m43.6^s$	0.4N	67.1E	33	5.1	Carlsberg Ridge
10*	1964 Aug 18	$15^h26^m11.9^s$	5.7N	57.9E	33	5.4	Carlsberg Ridge
11	1964 Nov 7	$18^h37^m43.7^s$	0.4N	100.1E	107	5.1	Sumatra
12	1964 Nov 21	$22^h40^m12.0^s$	4.9S	103.6E	33	5.4	Sumatra
13	1964 Nov 24	$10^h41^m33.5^s$	6.8S	107.4E	125	6.0	Java
14	1964 Dec 3	$03^h50^m01.2^s$	15.0S	66.8E	46	6.1	Mid Indian Rise
15	1965 Jan 5	$00^h51^m33.6^s$	7.3S	106.7E	89	5.3	Java

* Earthquakes relocated by USCGS using more stations than in the preliminary epicenter determination.

the Sumatra earthquake is larger. In both records we note that, in general, the early arrivals have shorter periods than the main P'_{DF} arrival but there is little evidence of dispersion. This agrees with the early observations made by Gutenberg.

The third and fourth traces in Figure 5 are events 4 and 3 recorded at TFO from

TABLE 3

RECORDING STATIONS USED

Event No.	Station Name	Epicentral Distance (deg)	Adjusted Epicentral Distance (deg)	Azimuth of Approach (deg)	Comment
1	TFO	140.01		74	Velocity filtered
	BMO	139.85		56	
	UBO	136.82		69	
	KN-UT	140.37		69	LRSM
	LC-NM	136.63		79	Velocity filtered, LRSM
	BX-UT	137.64		72	Velocity filtered, LRSM
2	TFO	137.04		305	
3	TFO	153.03	152.67	2	Velocity filtered
	WMO	149.92	149.77	27	
	KM-CL	152.05	151.50	349	LRSM
	KN-UT	150.31	150.20	358	Velocity filtered
	BX-UT	149.67	149.37	5	
	DR-CO	149.62	149.32	8	Velocity filtered, LRSM
4	TFO	153.71	152.87	122	Velocity filtered
	BMO	161.90	161.90	98	
	UBO	155.22	154.25	111	
	LC-NM	149.41	148.62	124	
	KN-UT	156.18	155.62	118	Velocity filtered
	BX-UT	154.02	153.12	116	Velocity filtered
	DR-CO	152.80	151.42	116	Velocity filtered
5	TFO	132.73		322	Velocity filtered
	WMO	137.53		339	
	WO-AZ	132.58		322	LRSM
	LC-NM	136.53		327	Velocity filtered
	SN-AZ	132.85		322	Velocity filtered, LRSM
	DR-CO	131.75		328	Velocity filtered
	JR-AZ	131.94		322	LRSM
6	TFO	133.82		320	
7	TFO	152.55		0	
8	TFO	149.75		128	
9	TFO	145.46	146.26	3	
	DR-CO	142.03	142.83	8	
	GE-AZ	145.93	146.88	4	
	LG-AZ	145.35	146.25	2	LRSM
10	TFO	138.93		17	
	GE-AZ	139.24		18	
	LC-NM	139.34		24	
	LG-AZ	138.88		16	
11	TFO	134.67		313	
12	TFO	136.43		304	
13	TFO	135.07		299	
14	TFO	160.72		6	
15	TFO	135.92		299	

epicenters at Prince Edward Island and the Chagos Archipelago. Both of these events are shallow focus earthquakes at an epicentral distance of about 153° from TFO. The multiplicity of events introduced by the shallow depth of focus is evident in these records. However, for the Prince Edward Island event the well defined pulse shapes, the time intervals of the events, and the information obtained from velocity filtering allow us to identify the main phases and their multiples. The identification of the various phases from the Chagos earthquake is somewhat less

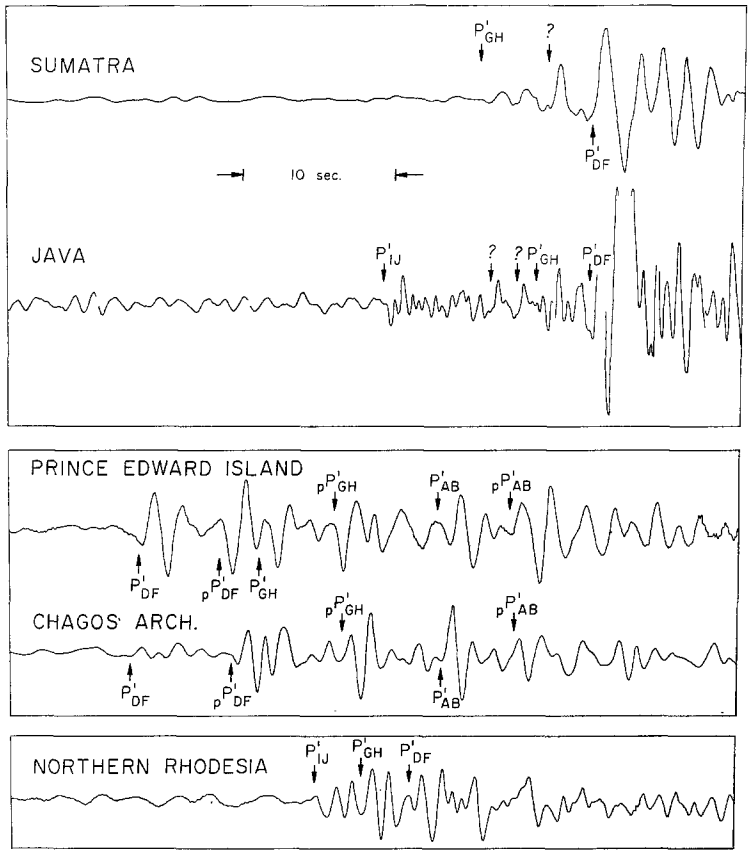

FIG. 5. Examples of core phases recorded at TFO for events no. 5, 13, 4, 3 and 1 in Table 2.

certain when only the same criteria are used. Part of this difficulty may be due to peculiarities in the source radiation pattern which causes the direct arrivals for some phases to be smaller than the reflected arrivals. However, upon including information obtained from the analysis of the Prince Edward Island shock, we can identify the reflections with some certainty and thus infer the presence of the direct arrivals. In both these records, we are not able to identity a distinct phase corresponding to P'_{IJ} .

The bottom trace in Figure 5 corresponds to event number 1 in Table 2. This is a shallow focus earthquake in Northern Rhodesia recorded at a distance of 140° from

TFO. Although many events are well defined on this record, the identification of the phases on the basis of amplitude or relative arrival time alone is difficult at this epicentral distance.

Velocity Filtering

The raw data for the events listed as "velocity filtered" in Table 3 were obtained in digital form on magnetic tape. The sampling interval was 0.05 sec. After correc-

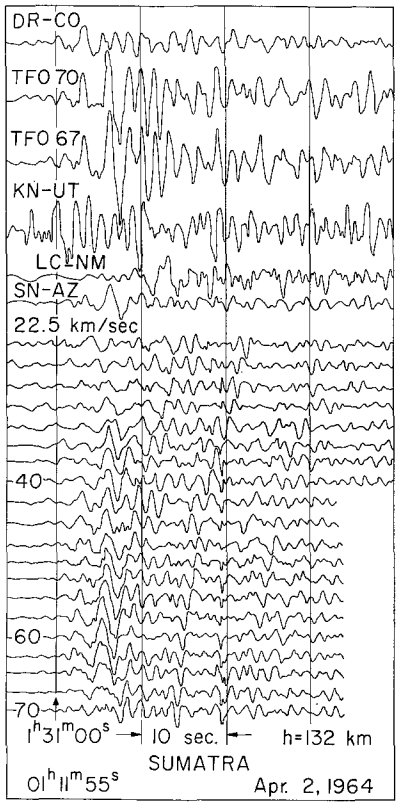

Fig. 6. The original records and the results of velocity filtering for the Sumatra earthquake of 2 April 1964.

tion for the individual instrument magnifications, the digital data were shifted in time and summed on a digital computer.

The time shift was determined by calculating the distances along the direction of approach from the individual stations to a reference point at TFO and then dividing by a selected apparent surface velocity. Summed records for apparent surface velocities ranging from 20 to 100 km/sec were obtained in steps of 2.5 km/sec. Although there were variations in the direction of approach at the individual LRSM stations because of their geographic separation, these variations did not appear to effect the results significantly. The velocity filtered records for the earthquakes located in Sumatra (5—Table 2), Northern Rhodesia (1) and Prince Edward

Island (4) are shown in Figures 6, 7 and 8. On the upper portion of each figure the records from the individual stations forming the array are shown. The lower portions of the figures show the velocity filtered results with TFO as a reference point.

For the Sumatra event (Figure 6), filtering with an apparent velocity of 55 km/sec emphasizes the large event occurring at TFO at $01^h31^m05^s$. This velocity is very near that predicted for P'_{DF} by all the proposed models. Therefore, using velocity filtering, as well as amplitude and arrival time we can unambiguously identify this event as P'_{DF}. The smaller event at $01^h30^m59^s$ cannot be identified on the basis of

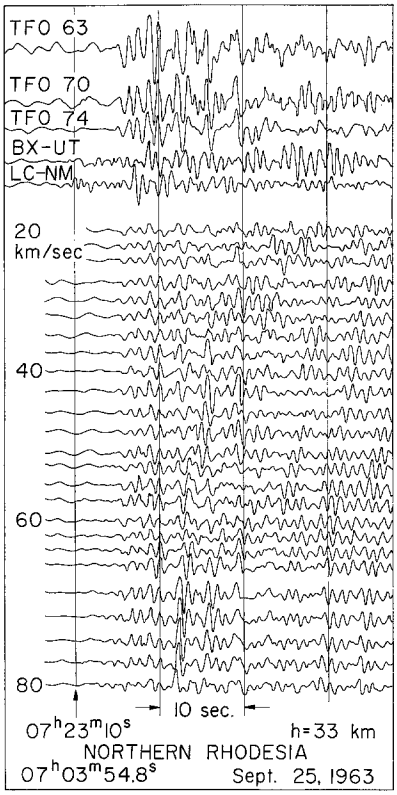

FIG. 7. The original records and the results of velocity filtering for the Northern Rhodesia earthquake of 25 September 1965.

apparent velocity alone, but its arrival time with respect to the established P'_{DF} branch can now be precisely determined.

In Figure 7 the results of velocity filtering the records from the earthquake in Northern Rhodesia are shown. TFO is at an epicentral distance such that the travel time curve is complex, and the relative arrival time and amplitudes of the phases are uncertain. The event occurring at $07^h23^m22^s$ is maximized for an apparent surface velocity of 70 km/sec. Since the predicted velocity for P'_{DF} at this epicentral distance is between 60 and 70 km/sec depending on the model chosen, this event has been identified as P'_{DF}. This identification is further supported by

adjusting all of the stations to P'_{DF} on the basis of those stations at shorter distances which record P'_{DF} unambiguously.

Figure 8 shows a similar display for the Prince Edward Island shock. The problem of phase identification for this earthquake is complicated by the presence of reflections from the free surface and the crust at the source and at the receivers. The epicentral distances at TFO and to DR-CO differ by less than 1° and yet the relative amplitudes of the first arrivals at the two stations are considerably different. Although we are not certain of the reason for this variation, it is particularly interesting since the TFO records from the Chagos Archipelago shock (Figure 5) are very similar to the DR-CO record for the Prince Edward Island shock.

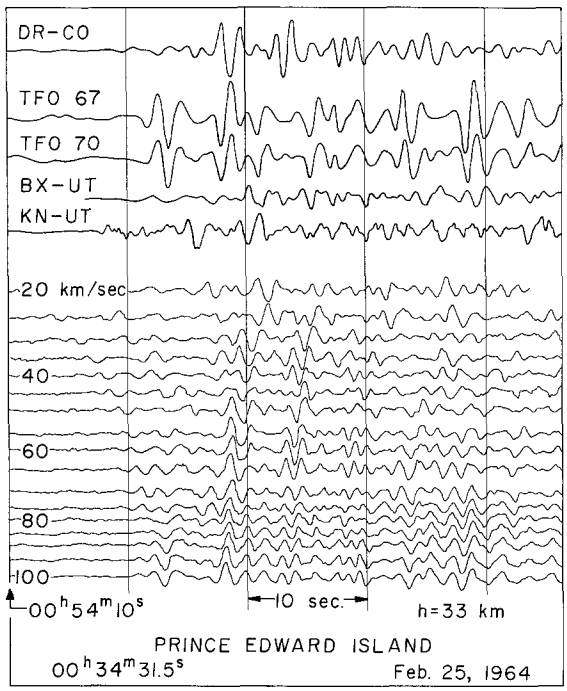

FIG. 8. The original records and the results of velocity filtering for the Prince Edward Island earthquake of 25 February 1964.

The following observations can be made from the velocity filtered records of the Prince Edward shock:

1) The first two phases recorded at TFO are P'_{DF} and pP'_{DF} with an apparent surface velocity of 90–100 km/sec.

2) The events occurring at $00^h54^m30^s$ and 35^s are a direct arrival and its surface reflection. They have apparent surface velocities ranging from 30 to 45 km/sec. The lack of precision in the measured apparent surface-velocity suggests that both P'_{IJ} and P'_{GH} and their multiples may be present. However, the evidence is far from conclusive because of the small number of stations used for velocity filtering. The apparent surface velocities of this event rule out the possibility that these are multiple events introduced by crustal layering.

3) The events occurring at $00^h54^m42^s$ and 47^s appear to be complex events composed of P'_{AB} and pP'_{AB} maximizing at apparent surface velocities of 20 to 25 km/sec, and crustal multiples and possibly phases similar to P'_{IJ} maximizing at higher velocities. Of these possibilities, only the events P'_{AB} and pP'_{AB} were identified.

Travel Time Curves

Once the phases were identified on the seismograms which were velocity filtered, the times were corrected to those of surface focus and plotted as conventional travel time curves (Figures 9 and 10). The times from the unfiltered records were also plotted using the velocity filtered records as a guide. At distances less than 140° the travel times of the phase with largest amplitude were adjusted to agree with the

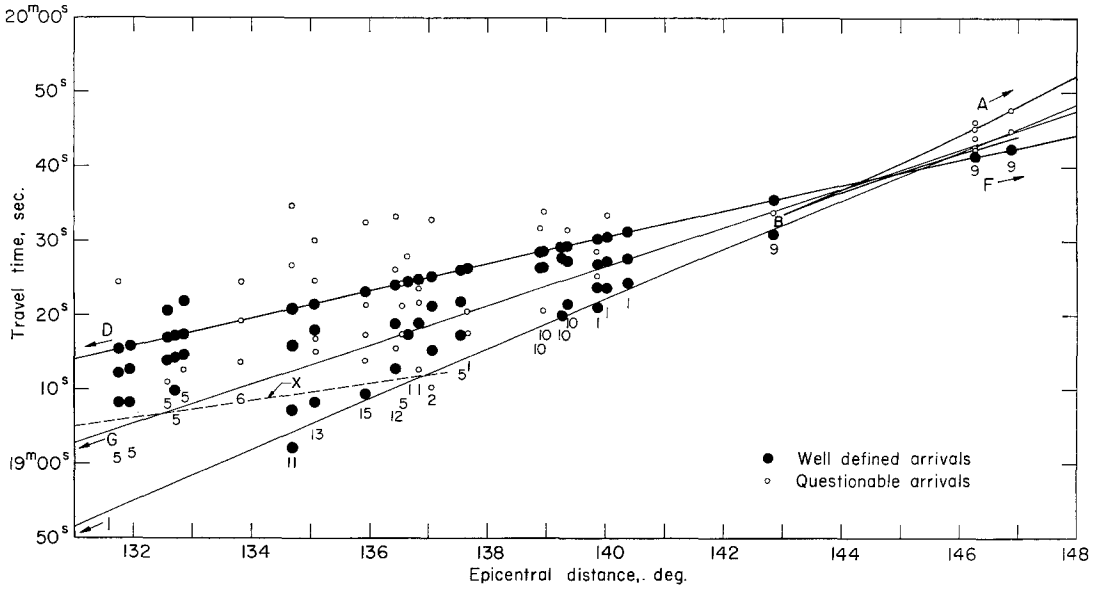

FIG. 9. Observed travel times (adjusted to the standard Jeffreys' curves) for *PKP* phases in the range 131° to 148°. The heavy solid line is the Jeffreys curve, the light solid lines are the precursors predicted by Adams and Randall, and the dashed line is the *X* branch of Hai.

Jeffreys' curve for P'_{DF}. At distances greater than 148°, the travel times and epicentral distances of the events were adjusted to allow the phases identified as P'_{DF} and P'_{AB} to agree with Jeffreys' travel time curves. The time shifts were only several seconds and the adjusted changes in epicentral distance were less than one degree. For those earthquakes recorded at many LRSM stations, these revisions were found to be consistent.

In Figure 9, there is a strong indication of two precursors to P'_{DF} in the epicentral range from 135° to 140°, but there is a noticeable gap of observational data at the critical distance of 132°. In the 135° to 140° range our observations would tend to support those of Adams and Randall although it is clear that more data, perhaps statistically tested, are required to discriminate between the proposed models of Bolt and Adams and Randall.

The data from 146° to 163° (Figure 10) support previous observations of Gutenberg, Bolt, Adams and Randall, and Hai regarding the presence of an intermediate branch P'_{GH}. In the range from 154°–156° there are two arrivals near 20^m10^s which we could not identify with certainty as either another phase or a crustal multiple. A similar observation may be made concerning the intermediate phases near 161°. These observations may indicate the presence of an additional branch to P'_{GH}.

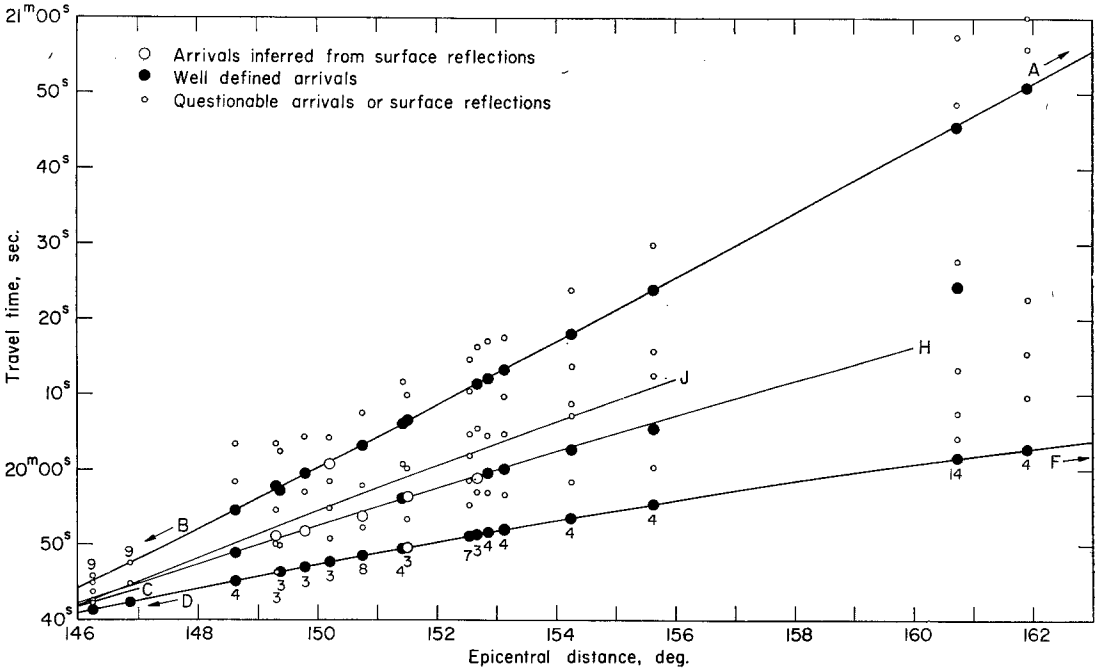

FIG. 10. Observed travel times (adjusted to Jeffreys' curves) for *PKP* phases in the distance range 146° to 163°. The heavy solid lines are the Jeffreys curves; the light solid lines are the branches predicted by Adams and Randall. The cusp at *C* is placed at the distance given by Jeffreys and Bullen.

CONCLUSIONS

Core phases, arising from the transition zone at the boundary of the inner core, were studied on seismograms recorded at the Tonto Forest array and many of the surrounding LRSM stations. Velocity filtering, in the form of time delaying and summation across the large array, was used to supplement conventional amplitude and travel time methods in the study of these core arrivals. Utilization of the apparent surface velocity is a useful technique when applied to the analysis of seismic core phases.

From this study we have concluded that there is a strong indication of two short period precursors to the main P'_{DF} arrival at distances less than 140° and the amplitudes of these phases are less than P'_{DF}. At least one of these precursors is an intermediate arrival to P'_{DF} and P'_{AB} at distances greater than 145°. The observed

apparent velocity of this arrival suggests that it is an extension of the P'_{GH} precursor observed at distances less than 140°. The amplitude of P'_{GH} is often equal to or greater than P'_{AB} and P'_{DF} at distances greater than 143°.

The phase P'_{IJ} is small at distances less than 140° but in some earthquakes examined, this phase was absent. Beyond 145° there are some indications that P'_{IJ} exists but the identifications of the arrivals are uncertain.

Our data appear to support most nearly the velocity solution for the core proposed by Adams and Randall (1964), although it is clear that more data in the epicentral distance range of 130° to 134° are required to discriminate between competing models. This study has indicated, however, that velocity filtering of core phases does provide valuable supplementary information. Even though absolute epicentral locations may not be known, the observed apparent velocities can be used for phase recognition and discrimination against unwanted signals. Future analyses, however, must correct for the effects of local crustal structure beneath the array.

Acknowledgments

The authors wish to thank Dr. S. T. Algermissen and the U. S. Coast and Geodetic Survey for their assistance in relocating some of the epicenters, and United Electrodynamics for supplying the digital tapes.

This research was supported by the Advanced Research Projects Agency and was monitored by the Air Force Office of Scientific Research under Contract AF-49(638)-1337.

References

Adams, R. D., and M. J. Randall (1963). Observed triplification of *PKP*, *Nature* **200**, 744–745.

Adams, R. D., and M. J. Randall (1964). The fine structure of the earth's core, *Bull. Seism. Soc. Am.* **54**, 1299–1313.

Bolt, B. A. (1962). Gutenberg's early *PKP* observations, *Nature*, **196**, 122.

Bolt, B. A. (1964). The velocity of seismic waves near the earth's center, *Bull. Seism. Soc. Am.* **54**, 191–208.

Gutenberg, B. (1957). The boundary of the earth's inner core, *Am. Geophys. Union Trans.* **38**, 750–753.

Gutenberg, B. (1958a). Caustics produced by waves through the earth's core, *Geophys. J.* **3**, 238–248.

Gutenberg, B. (1958b). Wave velocities in the earth's core, *Bull. Seism. Soc. Am.* **48**, 301–314.

Gutenberg, B. (1959). *Physics of the Earth's Interior*. Academic Press, 111–113.

Gutenberg, B., and C. F. Richter (1938). *P'* and the earth's core, *Mon. Not. R. A. S., Geophys. Suppl.* **4**, 363–372.

Hai, N. (1961). Propagation des ondes longitudinales dans le noyeau terrestre d'apres les seismes profonds de lles Fidji, *Ann. Geophys.* **17**, 60–66.

Hai, N. (1963). Propagation des ondes longitudinales dans le noyeau terrestre, *Ann. Geophys.* **19**, 285–346.

Jeffreys, H. (1939a). The times of the core waves, *Mon. Not. R. A. S., Geophys. Suppl.* **4**, 548–561.

Jeffreys, H. (1939b). The times of the core waves, *Mon. Not. R. A. S., Geophys. Suppl.* **4**, 594–615.

Lehmann, I. (1936). *P'*, *Publs. Bur. Central Seism. Intern. Trav. Sci.*, (A), **14**, 87–115.

Seismological Laboratory
California Institute of Technology
Pasadena, California
Division of Geological Sciences
Contribution No. 1357

Manuscript received August 2, 1965.